激光熔覆制备 Fe-Ti-Mo-C系复合涂层

王新洪[1,2]，　张　敏[3]，　邹增大[1]，　曲仕尧[1]
（1. 山东大学 材料液固结构演变与加工教育部重点实验室，济南　250061；
2. 山东大学 空间热物理研究中心，济南　250061；
3. 山东大学 机械工程学院，济南　250061）


王新洪

摘　要：采用钛铁、钼铁和石墨为激光熔覆粉末，利用激光多道搭接熔覆技术在碳钢基体上制备 Fe-Ti-Mo-C复合涂层. 利用 X射线衍射仪、场发射扫描电镜、电子探针对涂层的相结构和显微组织进行了研究. 用显微硬度计和滑动磨损试验机，对涂层的硬度和耐磨性能进行测试. 结果表明，涂层中原位生成了（Ti,Mo）C复合碳化物. （Ti,Mo）C呈面心立方结构，晶格常数略小于 TiC晶粒. 随着原材料中钼铁加入量的增加，涂层显微组织由铁素体、珠光体向马氏体转变，显微硬度和耐磨性增加，但抗裂性能降低.

关键词：复合碳化物；激光熔覆；显微组织；耐磨性能
中图分类号：TG159.9　文献标识码：A　文章编号：0253－360X（2010）12－0053－04

0　序　　言

激光具有快速熔凝、稀释率低、涂层与基体呈冶金结合、基材的热影响区以及变形小等特点，已成为材料表面改性技术的一种重要方法. 国内外学者已采用激光熔覆技术制备出外加颗粒或原位合成陶瓷相增强的金属基复合涂层，并对激光熔覆工艺进行了较为系统的研究[1－5].

文中曾采用 Fe-Ti30、石墨及铁基合金粉末作为熔覆材料，制备出原位合成的 TiC颗粒增强铁基激光涂层，制备的复合涂层与基材 45钢相比具有更好的硬度和耐磨性能[6,7]. 采用 Fe-Ti30粉末作为熔覆材料可以降低熔覆材料的成本，但 Fe-Ti30的加入量不宜过大，否则影响涂层成形性. 为了进一步提高涂层的硬度和耐磨性能，希望在熔覆材料中加入其它碳化物形成元素，以便生成 TiC与其它碳化物共同增强基体. 众所周知，过渡族元素 Mo是一种碳化物形成元素，既能在钢中析出弥散分布的 MoC或 Mo_2C碳化物质点，又能以固溶强化方式提高钢的强度. Shin Yao等人[8,9]在钴基 stellite堆焊材料中添加 Mo元素，发现堆焊层的硬度和耐磨性能得到显著提高. 此外，钼增大了钢的淬透性，提高了奥氏体的稳定性，促使生成马氏体组织.

文中将采用钛铁、钼铁、石墨及铁基合金为原材料，利用激光熔覆技术制备 TiC，MoC等颗粒增强铁基涂层，并对涂层的组织与性能进行研究.

1　试验方法

基体为 45钢，尺寸为 50 mm×30 mm×10 mm. 合金粉末为 Fe-Ti30、Fe-Mo70及石墨，为了改善涂层的成形，在粉末中加入少量的纯铁粉和 CaF_2. 按原子比 Ti∶C＝1∶1和 Mo∶C＝1∶1的配比设计 Ti，Mo元素和石墨的加入量. 为了分析 Fe-Mo合金的加入量对涂层组织与性能的影响，在合金粉末中保持 Fe-Ti30的加入量不变，分别加入 0%，5%，10%，15%和 17%（质量分数）的钼铁. 采用 VH－6型混料机将合金粉末混合均匀，然后将待熔覆材料预置于 45钢基体表面上，预涂层厚度约为 1.3 mm. 采用 5 kW横流 CO_2 激光器进行激光熔覆试验，光斑直径为 3 mm，扫描速度为 300 mm/min，功率为 2 500 kW，多道熔覆时搭接率为 33%.

利用 D/Max－Rc型 X射线衍射仪、SU－70型热场发射扫描电镜、JXA－8800R型电子探针，分别对涂层相结构、显微组织以及微区成分进行分析. 采用 HMV－2000型显微硬度计测试涂层的显微硬度，载荷为 1.96 N，加载时间为 15 s. 利用 M－2000型环块滑动磨损试验机对涂层的耐磨性进行分析，磨损载荷为 150 N，磨损时间为 25 min.

收稿日期：2009－08－28
基金项目：山东省自然科学基金资助项目（Z2006F07）

2 试验结果与分析

2.1 涂层的宏观形貌

图 1a为熔覆材料中添加 5% Fe-Mo的涂层宏观形貌. 由图 1a可以看出, 通过选择合适的激光熔覆工艺参数, 可以制备出成形良好、致密且无气孔和裂纹的涂层. 图 1b为涂层与基材的界面形貌, 由图 1b可以看出, 涂层底部在熔合区部位主要以树枝晶形式生长, 树枝晶的主干生长方向大致平行于熔池散热方向且呈现出以半熔化的基体晶粒为形核核心外延生长的特征, 从而表明涂层与基材已形成良好的冶金结合. 这种冶金结合有利于提高涂层与基材的结合强度.

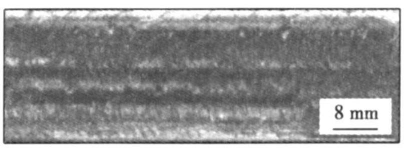

(a) 涂层表面形貌

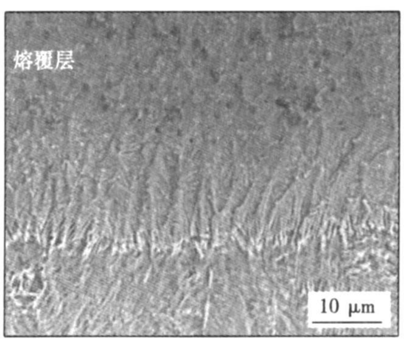

(b) 界面形貌

图 1 添加 5% Fe-Mo涂层宏观形貌及界面形貌
Fig. 1 Marco-morphology of clad coating

2.2 涂层的相结构与显微组织

图 2为添加 5% Fe-Mo的涂层 X射线衍射图谱. 由图 2可以看出, 涂层的相结构主要是由 TiC, α-Fe及 Fe_3C组成. 表明在激光热源的作用下 Fe-Ti与石墨反应生成了 TiC颗粒. 但在衍射图谱中没有发现 MoC或 Mo_2C, 其原因可能为 (1)由于涂层中反应生成 MoC或 Mo_2C的量非常少, 而在现有设备的检测精度下检测不到或被其它衍射峰所覆盖; (2)在激光热源的作用下熔覆材料通过原位反应先形成初生 TiC, 在随后的熔凝过程中 Mo元素以固溶的形式进入 TiC晶体, 取代钛而形成 (Ti, Mo) C复合碳化物. Kim, Lindahl等人[10,11]在制备 (Ti, Mo) C-Ni金属陶瓷时, 也发现这种现象. 研究结果表明添加钼后衍射图谱中虽然没有直接检测到 (Ti, Mo) C, 但发现 TiC(200)峰由 41.705°向更高角度 (41.75°)偏移, 并认为产生这种偏移现象的主要原因是由于钼固溶到 TiC中形成 (Ti, Mo) C. 而文中 TiC(200)的衍射角与标准卡中 TiC(200)相比也同样存在向高衍射角偏移这种现象, 即 TiC(200)的 2θ由标准的 41.705°增加到 41.96°, 因此, 表明涂层中也存在这种 (Ti, Mo) C的复合碳化物相.

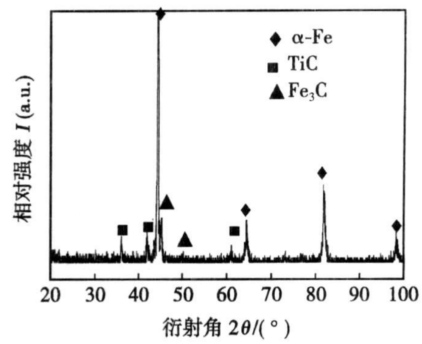

图 2 添加 5% Fe-Mo涂层的 X射线衍射图谱
Fig. 2 XRD pattern of coating with 5% Fe-Mo

图 3为碳化物的线扫描结果. 由图 3可见, 碳

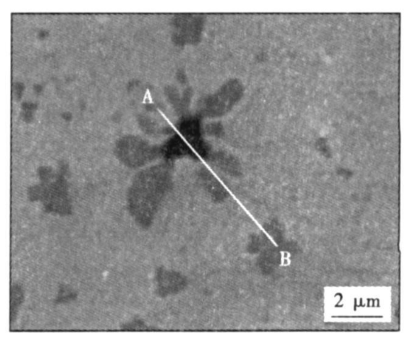

(a) 背散射电子形貌及扫描位置

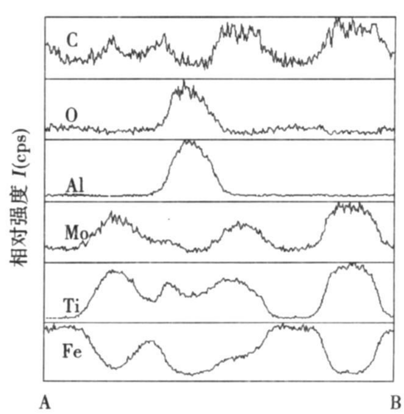

(b) 元素分布

图 3 添加 5% Fe-Mo涂层碳化物线扫描结果
Fig. 3 EPMA backscattered electron images and elemental line distribution of coating with 5% Fe-Mo

化物中同时富含 Ti, Mo及 C元素, 但贫 Fe元素. 由此可见, 这些碳化物为 (Ti, Mo) C的复合碳化物. 此外, 由图 3还可以看出, 碳化物呈花瓣状或块状均匀分布在涂层中, 部分碳化物中心部位呈现深黑色, 由从 A到 B线扫描分析表明, 中心部位富含 Al元素和 O元素, 因此, 判断这些黑色质点是 Al_2O_3. 形成 Al_2O_3 的主要原因是 Fe-Ti30中存在 8%左右的 Al元素, 而在激光熔覆过程中, 虽然采用了氩气保护, 但仍存在氧化气氛, 从而导致 Al元素氧化而形成 Al_2O_3.

图 4为不同含量 Fe-Mo的涂层显微组织形貌. 由图 4可以看出, 涂层中含有较多的碳化物, 且分布比较均匀, 这有利于涂层硬度和耐磨性能提高. 同时还发现随着 Fe-Mo合金加入量的增加, 涂层中基体组织发现明显的变化, 在不添加 Fe-Mo时, 涂层的基体组织主要是块状铁素体, 当加入 5%和 10%的 Fe-Mo合金时涂层中基体组织主要是珠光体, 而加入 15 %的 Fe-Mo合金后涂层的基体组织主要以片状马氏体为主, 但加入 17% 的 Fe-Mo后涂层出现裂纹. 产生裂纹的原因主要是一方面形成碳化物增加涂层变脆, 另一方面部分钼固溶到基体中使过冷奥氏体稳定性增加, 更容易向低温马氏体组织转变, 在热应力的作用下导致涂层开裂.

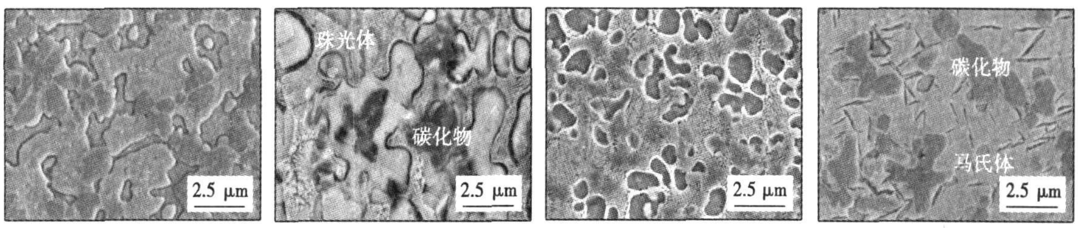

(a) 不添加Fe-Mo　(b) 添加5%Fe-Mo　(c) 添加10%Fe-Mo　(d) 添加15%Fe-Mo

图 4　Fe-Mo加入量对涂层组织的影响
Fig. 4　Effect of Fe-Mo on microstructure of coating

图 5为涂层中增强体的 TEM形貌及衍射斑点. 由图 5可见, 增强体为多边形, 增强体与基体界面结合良好, 且界面洁净, 无杂质和其它反应物, 这有利于提高碳化物颗粒与基体的结合强度. 由图 5b衍射斑点可知, 增强体为面心立方结构. 根据布拉格定律 $a = d\sqrt{h^2+k^2+l^2}$, 可计算出这种碳化物的晶格常数 a=0.431 8 nm, 与 TiC标准晶格常数 a=0.432 7 nm相比, 具有较小的晶格常数. 这主要是由于钼的原子半径为 0.139 nm, 而钛的原子半径为 0.147 nm, 这证明了部分 Mo元素溶入 TiC晶体中, 取代 Ti原子位置, 而导致晶格常数减小.

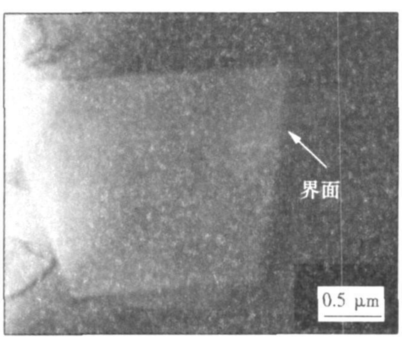

(a) TEM形貌

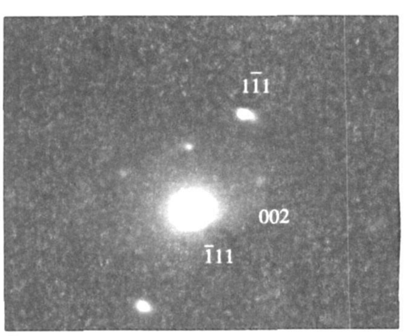

(b) 衍射斑点

图 5　涂层中增强体的 TEM形貌及衍射斑点
Fig. 5　TEM morphology of carbide in clad coating

2.3　涂层的硬度和耐磨性能

图 6和图 7分别为 Fe-Mo加入量对涂层显微硬

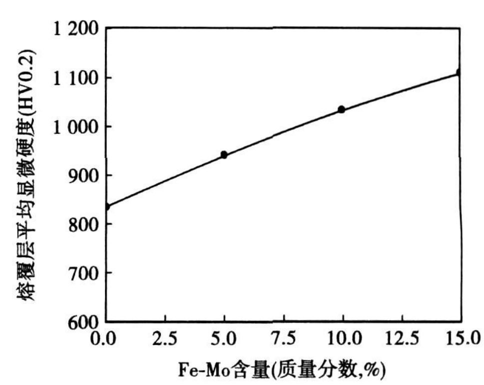

图 6　涂层表层平均显微硬度与 Fe-Mo加入量的关系
Fig. 6　Relationship between average microhardness of clad coating and content of Fe-Mo alloy

度和耐磨性能的影响. 由图可以看出,随着 Fe-Mo加入量的增加,涂层的硬度和耐磨性增加. 这主要是由于 Mo元素的增加促进了碳化物的形成,同时 Mo元素的固溶作用,使涂层的基体硬度也得到提高,从而使涂层具有更好的耐磨性能.

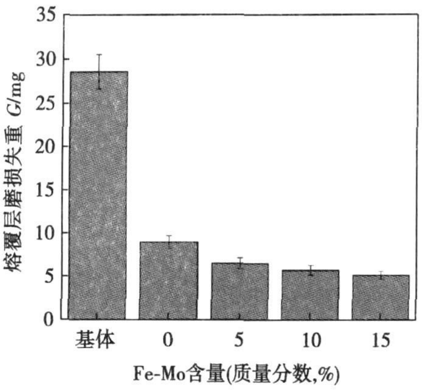

图 7 Fe-Mo加入量对涂层磨损失重的影响

Fig. 7 Effect of Fe-Mo on wear mass loss of clad coating

3 结 论

(1)采用激光熔覆技术,在碳钢板上制备出原位自生的 (Ti, Mo) C复合碳化物增强铁基涂层.

(2) (Ti, Mo) C呈花瓣状或块状均匀分布于基体中,其晶格结构仍保持 TiC晶体的面心立方结构,但晶格常数略小于 TiC晶体.

(3)加入 Fe-Mo后涂层的硬度和耐磨性显著提高. 随着 Fe-Mo加入量的增加,基体组织由铁素体向珠光体、马氏体转变,但抗裂性能降低.

参考文献:

[1] 杜宝帅, 李清明, 王新洪, 等. 激光熔覆原位自生 TiC-VC颗粒增强 Fe基金属陶瓷涂层[J]. 焊接学报, 2007, 28(4): 65-68.
Du Baoshuai, Li Qingming, Wang Xinhong, et al. In situ synthesis of TiC-VC particles reinforced Fe-based metal matrix composite coating by laser cladding[J]. Transactions of the China Welding Institution, 2007, 28(4): 65-68.

[2] Sing A, Dahotre N B. Laser in-situ synthesis of mixed carbide coating on steel[J]. Journal of Materials Science, 2004, 39(14): 4553-4560.

[3] Du Baoshuai, Zou Zengda, Wang Xinhong, et al. Laser cladding of in situ TiB2/Fe Composite coating on steel[J]. Apply Surface Science, 2008, 254(20): 6489-6494.

[4] Meng Q W, Geng L, Zhang B Y. Laser cladding of Ni-based composite coatings onto Ti6Al4V substrate with preplaced B4C + NiCrBSi powders[J]. Surface and Coatings Technology, 2006, 200(16/17): 4923-4928.

[5] 张锦英, 马明星, 刘文今. 钒、钛对激光熔覆铁基原位生成颗粒增强复合涂层组织的影响[J]. 金属热处理, 2003, 28(8): 1-4.
Zhang Jinying, Ma Mingxing, Liu Wenjin. Influence of V and Ti on the microstructure of in-situ particles reinforced Fe-based composite coating by laser cladding[J]. Heat Treatment of Metals, 2003, 28(8): 1-4.

[6] Qu Shiyao, Wang Xinhong. Microstructure and wear properties of Fe-TiC surface composite coating by laser cladding[J]. Journal Materials Science, 2008, 43(5): 1546-1551.

[7] Wang X H, Qu S Y, Du B S, et al. In situ synthesised TiC particles reinforced Fe-based composite coating produced by laser cladding[J]. Materials Science and Technology, 2009, 25(3): 388-392.

[8] Shin Jong Choul, Doh Jung Man, Yoon Jin Kook, et al. Effect of molybdenum on the microstructure and wear resistance of cobalt-base Stellite hardfacing alloys[J]. Surface and Coatings Technology, 2003, 168(2/3): 117-126.

[9] Yao M X, Wu J B C, Xie Y. Wear, corrosion and cracking resistance of some W- or Mo-containing Stellite hardfacing alloys[J]. Materials Science and Engineering A, 205, 407(1/2): 234-244.

[10] Kim Young kwan, Shim Jae hyeok, Cho Young whan, et al. Mechanochemical synthesis of nanocomposite powder for ultrafine (Ti, Mo) C-Ni cermet without core-rim structure[J]. International Journal of Refractory Metals & Hard Materials, 2004, 22(4/5): 193-196.

[11] Lindahl P. Microstructure of cermets[D]. Goteborg: Chalmers University of Technology, 1995.

作者简介: 王新洪, 男, 1969年出生, 博士, 教授. 主要从事材料表面改性、新材料焊接工艺研究, 获省部级科技进步奖 5项. 发表论文 70余篇.
Email: xinhongwang@sdu.edu.cn

WANG Feng, SONG Yonglun, ZHANG Jun (College of Mechanical and Electrical Engineering, Beijing University of Technology, Beijing 100124, China). p 37—40, 44

Abstract: The influence of welding parameters (pressure and current) on the size of nugget and heat-affect zone is obtained by analysing the microstructure of the nugget of the high-strength aluminum spot welding, the correlation between the parameters and the microstructure is obtained too, and the detailed influence of the little variation of the welding parameters and the less distinct change of the signals on welding nugget quality is observed, which lay a foundation for the further study of precise control of the spot welding process. The building model and the simulation of spot welding are achieved through finite element analysis software SYSWELD, and the relationship between the electrode pressure, welding current and nugget size is studied respectively.

Key words: high-strength aluminum spot welding; microstructure analyzing; finite element simulation

Testing study on SW-CCT diagram of 12Cr1MoV steel

HU Yanhua, CHEN Furong, XIE Ruijun, LI Haitao (College of Materials Science and Engineering, Inner Mongolia University of Technology, Hohhot 010051, China). p 41—44

Abstract: Temperature was selected as variable to study phase transformation in weld metal of 12Cr1MoV steel and realized in-situ detection of temperature in weld metal. The maximum temperature and cooling rates during welding were acquired to form the simulation technology of 12Cr1MoV steel in weld metal, and the SW-CCT diagram of 12Cr1MoV steel were obtained by the thermal simulation equipment with extracted cooling rates. When the average cooling rate of $t_{8/3}$ is under 1.7 ℃/s, the microstructure in weld metal of 12Cr1MoV steel is ferrite (F) + perlite (P) + bainite (B); under 4.7 ℃/s, the microstructure is P+B; under 33 ℃/s, the microstructure is B; over 33 ℃/s, the microstructure is martensite (M). The optical microstructures of typical cooling rates are coincident with the test results of SW-CCT. The Vikers hardness increases with the increasing of cooling rates.

Key words: 12Cr1MoV steel; weld metal; SW-CCT diagram

Experimental investigation on controlling welding hot crack with welding with trailing rotating extrusion

LI Jun, YANG Jianguo, TAN Xing, FANG Hongyuan (State Key Laboratory of Advanced Welding Production Technology, Harbin Institute of Technology, Harbin 150001, China). p 45—48

Abstract: The basic principle of welding with trailing rotating extrusion (WTRE) and its control effect in mitigating welding distortion are introduced. The impact of WTRE on welding hot crack of 2A12T4 aluminum alloy is investigated and analyzed. Experimental results show that with proper technological parameters, WTRE can inhibit the initiation and propagation of welding hot cracks effectively. The distance between extrusion tool and welding torch as well as the vertical force acting on the weldment are key technological parameters determining the control effect of welding hot cracking. WTRE method controls welding hot crack based on the binding to hot cracks at arc-starting end and the restraint action to externally expanded deformation of weldments.

Key words: welding with trailing rotating extrusion; aluminum alloy; welding; hot crack

Frictional and wear performance of WC-12Co/MoS_2 composite coatings by detonation-gun sprayed

ZHANG Song, ZHANG Kaixiang, HU Fang, ZHANG Chunhua, YAN Yonggen[2] (1. School of Materials Science and Engineering, Shenyang University of Technology, Shenyang 110870, China; 2. Baoshan Iron & Steel Co., Ltd., Shanghai 201900, China). p 49—52

Abstract: To further improving the wear resistance of the WC-12Co coatings, different proportions of MoS_2 powders were added into the WC-12Co powders and a series of the WC-12Co/MoS_2 composite coatings were prepared on the Q235 steel by detonation-gun spraying. The morphology, microstructure, microhardness, friction and wear performance, and wear behavior of the WC-12Co/MoS_2 composite coatings were investigated by optical microscope, scanning electron microscopy, X-ray diffraction, microhardness tester and wear tester, separately. The results showed that the MoS_2 powders were evenly dispersed in the WC-12Co coatings. When the content of MoS_2 was 2% (wt%), the hardness and density of WC-12Co/MoS_2 composite coating were changed little, but the friction coefficient and wear rate were significantly decreased by 50% and 33% in contrast with those of the WC-12Co coatings, respectively. Both of the friction coefficient and wear rate of the WC-12Co/MoS_2 composite coatings were risen gradually by further increased the content of MoS_2 in the WC-12Co coating.

Key words: detonation-gun spraying; WC-12Co; MoS_2 composite coatings; wear performance

Fabrication of Fe-Ti-Mo-C composite coating by laser cladding

WANG Xinhong[1,2], ZHANG Min, ZOU Zengda, QU Shiyao (1. Key Laboratory for Liquid-Solid Structural Evolution and Processing of Materials, Ministry of Education, Shandong University, Jinan 250061, China; 2. Institute of Thermal Science and Technology, Shandong University, Jinan 250061, China; 3. School of Mechanical Engineering, Shandong University, Jinan 250061, China). p 53—56

Abstract: Fe-Ti-Mo-C composite coatings were deposited on the steel by laser melting mixture of Fe-Ti, Fe-Mo and graphite powders. The phase structure and microstructure of the coatings were investigated by X-ray diffraction, field emission scanning electron microscope and electron probe micro-analyzer. Meanwhile, the microhardness and wear properties of the coatings were also tested by means of micro Vickers and block-on-ring wear testing machine. The results showed that (Ti, Mo) C multiple carbides were formed during laser cladding process. (Ti, Mo) C carbide has typically faceted feature, but the lattice pattern of (Ti, Mo) C carbide is somewhat less than that of TiC. With an increasing of addition of Fe-Mo, the microhardness and wear resistance of the coatings increased, but the crack resistance of the coatings decreased.

Key words: multiple carbide; laser cladding; microstructure; wear properties